

Coupling of order parameter and spin fluctuations in underdoped high- T_c cuprates

T. Dahm,* D. Manske, and L. Tewordt

Abteilung für Theoretische Festkörperphysik, Universität Hamburg, Jungiusstrasse 11, D-20355 Hamburg, Germany

(Received 12 February 1997)

We calculate self-consistently the spin and $d_{x^2-y^2}$ -wave order-parameter fluctuations (OPFL's) above T_c within an extension of the FLEX (fluctuation exchange) approximation for the two-dimensional Hubbard model. The quasiparticle interaction due to OPFL's can compete with that due to spin fluctuations for temperatures near T_c and short pairing correlation lengths like those in the cuprates. The coupling of these fluctuations via self-energy renormalization leads to a suppression of T_c and to a decrease of the dynamical spin susceptibility for decreasing T below a crossover temperature $T_* > T_c$. The temperature T_* increases while T_c decreases with increasing strength of OPFL's or decreasing doping. The resulting neutron-scattering intensity and NMR relaxation rates $1/T_1$ and $1/T_{2G}$ decrease below T_* for decreasing T . This agrees qualitatively with the observed spin gap behavior in the underdoped high- T_c cuprates. [S0163-1829(97)01122-3]

I. INTRODUCTION

A number of physical quantities in the normal state of high- T_c cuprates exhibits quite unusual properties in the underdoped regime. We concentrate in this paper on those quantities which are determined by the dynamical spin susceptibility $\chi(\mathbf{q}, \omega)$ for \mathbf{q} near the antiferromagnetic wave vector $\mathbf{Q} = (\pi, \pi)$. These are in particular the ^{63}Cu spin-lattice relaxation rate $1/T_1$ given by $1/T_1 T = \sum_q |A_q|^2 \lim_{\omega \rightarrow 0} \chi(\mathbf{q}, \omega) / \omega$ and the inelastic neutron-scattering intensity which is proportional to $\text{Im}\chi(\mathbf{q}, \omega)$. In the overdoped regime $1/T_1 T$ increases continuously as T decreases down to T_c while in the underdoped regime $1/T_1 T$ passes through a maximum at a temperature T_* for decreasing T (see Ref. 1). These results are fully corroborated by inelastic neutron-scattering data where in the underdoped regime $\text{Im}\chi(\mathbf{Q}, \omega)$ at fixed small ω ($\hbar\omega = 10$ or 15 meV) passes through a maximum at T_* for decreasing T (see Ref. 2). It has been suggested that the decrease of $1/T_1 T$ and the neutron-scattering intensity below T_* are a signature of the opening of a spin pseudogap in the magnetic excitations.²

The third important quantity which is determined by the dynamical susceptibility is the spin-echo decay rate $1/T_{2G} \propto [\sum_q \text{Re}\chi(\mathbf{q}, 0)]^{1/2}$. In the overdoped regime the ratio $T_1 T / T_{2G}^2$ is almost temperature independent which corresponds according to scaling arguments to a dynamical exponent $z = 2$ where the spin excitations are relaxation modes.³ In the underdoped regime the ratio $T_1 T / T_{2G}^2$ is constant down to a crossover temperature T_{cr} , and then it increases with decreasing T . The other significant ratio is $T_1 T / T_{2G}$ which for decreasing T decreases down to T_{cr} , then becomes constant between T_{cr} and T_* , and finally increases below T_* (see Ref. 1). The relationship $T_1 T / T_{2G} = \text{const}$ in the temperature range between T_{cr} and T_* corresponds to a dynamical scaling exponent $z = 1$ which occurs in the quantum-disordered regime.³ Recently, a counterpart to the spin pseudogap in nuclear magnetic resonance (NMR) and neutron scattering has been found, namely, a quasiparticle gap with d -wave symmetry above T_c in angle-resolved photoemission (ARPES) experiments on underdoped

$\text{Bi}_2\text{Sr}_2\text{CaCu}_2\text{O}_{8+\delta}$ (Bi2212) compounds.⁴ It has been proposed that the physical origin of this normal state gap is preformed d -wave pairs without long-range phase coherence.^{5,6}

In this paper we show that another mechanism may be responsible for the suppression of the spin fluctuations and of T_c , namely, coupling to d -wave order parameter fluctuations which are treated in analogy to the classical Aslamazov-Larkin theory.⁷ Spin-triplet p -wave order-parameter fluctuations below T_c have been observed in superfluid ^3He and have been calculated from parquet equations for the T matrices in the particle-particle and particle-hole channels.⁸ Particle-hole and particle-particle scattering together were considered also in the FLEX (fluctuation exchange) approximation for the two-dimensional (2D) Hubbard model.⁹ The effect of particle-particle scattering is to reduce T_c for $d_{x^2-y^2}$ -wave pairing which is obtained from the FLEX approximation for spin-fluctuations alone.¹⁰⁻¹²

In this paper we generalize the Eliashberg equations of Ref. 12 by taking into account, beside the self-energy contribution due to particle-hole scattering, the self-energy Σ' due to particle-particle scattering T' . The particle-particle scattering matrix T' is calculated in the ladder approximation with the full spin fluctuation interaction. This yields an analogous expression to the Ginzburg-Landau-Gorkov (GLG) expression for the order-parameter fluctuation propagator.⁷ In particular, the pairing instability in T' is determined by the denominator expression $T' \propto [|T - T_c| / T_c + \xi_0^2 q^2 - i\omega\tau]^{-1}$ where ξ_0 is the superconducting coherence length at $T = 0$ and τ is the relaxation time due to pair breaking. The effect of T' is to enhance the quasiparticle damping and, in turn, to suppress the dynamical spin susceptibility. This effect becomes very large as T tends towards T_c because ξ_0 and τ are relatively small for the high- T_c cuprates. The result is that the neutron-scattering intensities $\text{Im}\chi(\mathbf{q}, \omega)$, $1/T_1 T$, and $1/T_{2G}$ exhibit for decreasing T a pronounced crossover at $T_* > T_c$ to spin pseudogap behavior.

In Sec. II we derive the order-parameter fluctuation propagator and the generalized FLEX approximation equa-

tions for the 2D Hubbard model. The results for the dynamical spin susceptibility, neutron scattering intensity, and NMR relaxation rates are presented and discussed in Sec. III. Section IV is devoted to the conclusions.

II. ORDER-PARAMETER FLUCTUATION PROPAGATOR AND FLEX APPROXIMATION FOR 2D HUBBARD MODEL

In the previous FLEX (fluctuation exchange) approximation for the 2D Hubbard model¹⁰⁻¹² the interaction between quasiparticles due to exchange of spin fluctuations has been taken into account. Here we generalize this theory by including the interaction due to exchange of order-parameter fluctuations. We are led by the expression for the particle-particle scattering matrix T' which has been obtained from Ginzburg-Landau-Gorkov (GLG) theory⁷ (we omit here the coupling term between neighboring layers):

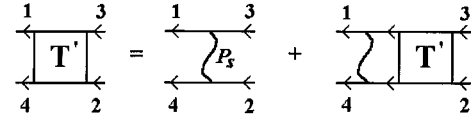
$$T'(\mathbf{k}_1, \mathbf{k}_3; \mathbf{q}, \nu) = - \frac{\psi(\mathbf{k}_1)\psi^*(\mathbf{k}_3)}{N[(|T-T_c|)/T_c + \xi_0^2 q^2 - i\nu\tau]}. \quad (1)$$

The T' in Eq. (1) refers to the scattering of a pair of particles with momenta $\mathbf{k}_3 + (\mathbf{q}/2)$, $(\mathbf{q}/2) - \mathbf{k}_3$ and total energy ν to a pair $\mathbf{k}_1 + (\mathbf{q}/2)$, $(\mathbf{q}/2) - \mathbf{k}_1$, ν . The function ψ is the basis function for the ‘‘embryonic’’ superconducting state above T_c ; here $\psi(\mathbf{k}) = \cos(k_x) - \cos(k_y)$ for d -wave pairing, ξ_0 is the superconducting coherence length at $T=0$, and τ is the relaxation time. The GLG expressions⁷ for ξ_0 and τ involve the tight-binding function $\epsilon(\mathbf{k})$ and the pairing function $\psi(\mathbf{k})$.

In analogy to Eq. (1) we have calculated $T'(k_1, k_3; q = k_1 + k_4)$ ($k \equiv \mathbf{k}, i\omega_n; q \equiv \mathbf{q}, i\nu_m$) in the ladder approximation for the full pairing interaction $P_s(k_1 - k_3) = (3/2)U^2\chi(k_1 - k_3)$ where U is the on-site Coulomb repulsion and χ is the dynamical spin susceptibility¹² (see Fig. 1). The resulting Bethe-Salpeter equation is the following:

$$T'(k_1, k_3; q = k_1 + k_4) = P_s(k_1 - k_3) - T \sum_{k'_1} P_s(k_1 - k'_1) \times G(k'_1)G(q - k'_1)T'(k'_1, k_3; q). \quad (2)$$

For $q=0$ the homogeneous part of this integral equation corresponds to the linearized gap equation whose eigensolutions $\phi_\lambda(k)$ and eigenvalues λ are determined by¹²



$$\sum'(\mathbf{k}) = \begin{array}{c} \mathbf{k} \quad \mathbf{k} \\ \leftarrow \quad \leftarrow \\ \text{---} \text{---} \text{---} \text{---} \\ \leftarrow \quad \leftarrow \\ \mathbf{k}' \end{array}$$

FIG. 1. Bethe-Salpeter equation for particle-particle scattering matrix T' in the ladder approximation with full pairing interaction $P_s = (3/2)U^2\chi$ (wavy line) and self-energy contribution Σ' arising from T' (the solid lines are the dressed particle propagators).

$$\lambda \phi_\lambda(k_1) = -T \sum_{k'_1} P_s(k_1 - k'_1)G(k'_1)G(-k'_1)\phi_\lambda(k'_1). \quad (3)$$

This suggests an expansion of T' in terms of basis functions ϕ_λ , yielding

$$T'(k_1, k_3; q=0) = \sum_\lambda \frac{p_\lambda \phi_\lambda(k_1)\phi_\lambda^*(k_3)}{1 - \lambda(T)}, \quad (4)$$

$$p_\lambda = \int dk_1 \int dk_3 \phi_\lambda^*(k_1)P_s(k_1 - k_3)\phi_\lambda(k_3). \quad (5)$$

Since the largest eigenvalue λ is the λ_d for $d_{x^2-y^2}$ -wave pairing,¹² we keep in the following only the leading term of Eq. (4) for $\lambda = \lambda_d$ and $\phi_\lambda = \phi_d$. The coupling constant p_d is calculated from Eq. (5) by approximating the spin fluctuation interaction P_s by δ -function peaks in wave vector \mathbf{q} and frequency ν :

$$\text{Re}P_s(\mathbf{q}, \nu) \approx 4\pi^2 \gamma(\Delta q)^2 (3/2)U^2 \text{Re}[\chi(\mathbf{Q}, 0)\delta(\nu)\delta(\mathbf{q} - \mathbf{Q})]. \quad (6)$$

Here, Δq is the half-width of the peak of $\text{Re}\chi(\mathbf{q}, 0)$ around $\mathbf{q} = \mathbf{Q} = (\pi, \pi)$, and γ is the half-width of the peak of $\text{Re}\chi(\mathbf{Q}, \nu)$ around $\nu = 0$. Making use of the fact that the eigensolution is normalized to unity and has the property $\phi_d(\mathbf{k} - \mathbf{Q}, \omega) = -\phi_d(\mathbf{k}, \omega)$ we obtain from Eqs. (5) and (6)

$$p_d = -4\pi^2 \gamma(\Delta q)^2 (3/2)U^2 \text{Re}\chi(\mathbf{Q}, 0). \quad (7)$$

The next step is to derive T' for finite pair momentum \mathbf{q} and energy ν . The corresponding correction terms are obtained from Eq. (2) by expanding the pair propagator $G(k)G(q-k)$ in powers of \mathbf{q} up to second order and in powers of ν up to first order. In analogy to Ref. 7 we obtain from Eq. (2) with the help of Eq. (6)

$$T'(\mathbf{k}_1, \omega_1; \mathbf{k}_3, \omega_3; \mathbf{q}, \nu) = - \frac{g}{4N} \frac{\phi_d(\mathbf{k}_1, \omega_1)\phi_d^*(\mathbf{k}_3, \omega_3)}{[(1 - \lambda_d) + (g/4)\xi_0^2 q^2 - i(g/4)\tau\nu]}, \quad (8)$$

$$\xi_0^2 = \frac{1}{N} \int_{-\infty}^{+\infty} d\omega \sum_{\mathbf{k}} |\phi_d(\mathbf{k}, \omega)|^2 \frac{1}{8} \{ [\partial \epsilon(\mathbf{k}) / \partial k_x]^2 + [\partial \epsilon(\mathbf{k}) / \partial k_y]^2 \} T_c \sum_{\omega_n(T_c)} \left[\frac{4\omega_n^2}{[\omega_n^2 + \epsilon(\mathbf{k})^2]^3} - [\omega_n^2 + \epsilon(\mathbf{k})^2]^{-2} \right], \quad (9)$$

$$\tau = \frac{1}{N} \int_{-\infty}^{+\infty} d\omega \sum_{\mathbf{k}} |\phi_d(\mathbf{k}, \omega)|^2 (\pi/2) \delta[2\epsilon(\mathbf{k}) - \nu] [\tanh(\nu/4T_c)/(\nu/2)]. \quad (10)$$

The expressions for ξ_0^2 and τ in Eqs. (9) and (10) correspond to the GLG expressions given in Ref. 7. They are approximately equal to $\xi_0^2 \approx [7\zeta(3)/48](v_F/\pi T_c)^2$ and $\tau = \pi/8T_c$. The dimensionless coupling constant g is proportional to $|p_d|$ in Eq. (7):

$$g = -p_d/\pi t = 4\pi\gamma(\Delta q)^2(3/2)(U/t)^2 \text{Re}[\chi(\mathbf{Q}, 0)t]. \quad (11)$$

Here, t is the nearest-neighbor hopping energy and $\bar{N} = 1/4\pi t$ is the average density of states.

We come now to the calculation of the self-energy contribution $\Sigma'(k)$ due to the T' matrix. This is shown diagrammatically in Fig. 1 and is given by

$$\begin{aligned} \Sigma'(\mathbf{k}, i\omega_n) = & T \sum_{\omega'_n} \sum_{\mathbf{k}'} T'(k, k; \mathbf{q} = \mathbf{k} + \mathbf{k}', i\nu_m = i\omega_n \\ & + i\omega'_n) G(\mathbf{k}', i\omega'_n). \end{aligned} \quad (12)$$

We now introduce in Eq. (12) the spectral representation of the T' matrix with respect to the Matsubara frequency $i\nu_m = i2m\pi T$ and the spectral representation of the Green's function G with respect to $i\omega'_n = i\nu_m - i\omega_n$. Then the summation over ω'_n , or ν_m , yields the function $I(i\omega_n, \Omega, \omega')$ given in Ref. 12. Then we carry out the analytical continuation $i\omega_n \rightarrow \omega + i\delta$, separate Σ' into the odd- and even- ω parts $\omega(1-Z)$ and ξ , and finally add the self-energy contribution due to the spin fluctuation interaction P_s (see Ref. 12). In this way we obtain the following generalized Eliashberg equations:

$$\begin{aligned} \omega[1 - Z(\mathbf{k}, \omega)] = & \sum_{\mathbf{k}'} \int_0^{\infty} d\Omega [|\phi_d(\mathbf{k}, \omega)|^2 K(\mathbf{k} - \mathbf{k}', \Omega) \\ & + P_s(\mathbf{k} - \mathbf{k}', \Omega)] \int_{-\infty}^{+\infty} d\omega' \\ & \times I(\omega, \Omega, \omega') A_0(\mathbf{k}', \omega'), \end{aligned} \quad (13)$$

$$K(\mathbf{q}, \Omega) = \frac{g}{4\pi\bar{N}} \frac{(g/4)\tau\Omega}{[(1 - \lambda_d) + (g/4)\xi_0^2 q^2]^2 + [(g/4)\tau\Omega]^2}. \quad (14)$$

The other Eliashberg equation for the energy shift function $\xi(\mathbf{k}, \omega)$ is obtained from Eq. (13) by changing the sign in front of the first term $|\phi_d|^2 K$ and by replacing the spectral function A_0 by $A_3(\mathbf{k}', \omega')$. The spin fluctuation interaction P_s , the spectral functions A_0 and A_3 , and the kernel I are given in Ref. 12. It should be noticed that the spin fluctuation interaction $P_s = (3/2)U^2\chi_0(1 - U\chi_0)^{-1}$ is calculated from the irreducible spin susceptibility χ_0 which is determined by the quasiparticle spectral function $N(\mathbf{k}, \omega) = A_0 + A_3$. The latter functions are renormalized by the self-energies $\omega(1-Z)$ and $\xi(\mathbf{k}, \omega)$. Equation (13) for $\omega[1 - Z(\mathbf{k}, \omega)]$ and the corresponding one for $\xi(\mathbf{k}, \omega)$ and the eigenvalue for

λ_d and $\phi_d(\mathbf{k}, \omega)$ are calculated self-consistently together with the interactions P_s (see Ref. 12) and K [see Eq. (14)].

III. RESULTS FOR DYNAMICAL SPIN SUSCEPTIBILITY AND NMR RELAXATION RATES

We have solved numerically Eq. (13) for the quasiparticle self-energy component $\omega[1 - Z(\mathbf{k}, \omega)]$ and the corresponding equation for the component $\xi(\mathbf{k}, \omega)$, with order-parameter fluctuation K [see Eq. (14)] and spin fluctuation interaction $P_s = (3/2)U^2\chi$. The kernel I , the spectral functions A_0 and A_3 and the interaction P_s are given in Ref. 12. In addition to the equations for $\omega(1-Z)$ and ξ , we have solved numerically the eigenvalue equation for the gap function $\phi_d(\mathbf{k}, \omega)$ with eigenvalue λ_d (see Ref. 12). The superconducting transition temperature T_c is given by that temperature where, for decreasing T , the eigenvalue $\lambda_d(T)$ passes through unity. It should be emphasized that λ_d and ϕ_d are calculated self-consistently which takes into account the renormalization of the order-parameter by the spin fluctuations. On the other hand, the spin fluctuations are renormalized by the order parameter fluctuations since the irreducible spin susceptibility χ_0 is calculated from the spectral function $N(\mathbf{k}, \omega) = A_0 + A_3$. The latter function is determined self-consistently from the Eliashberg equations [see Eq. (13)] containing the interactions P_s and K .

We consider here a tight-binding band $\epsilon(\mathbf{k})$ with nearest-neighbor hopping whose 2D Fermi line is similar to that of the YBaCuO and Bi2212 compounds.¹² The band filling is varied by varying the chemical potential μ which has been included in $\epsilon(\mathbf{k})$. For the on-site Coulomb repulsion we take $U = 6t$ and $\mu = -0.8$, yielding a renormalized band filling $n = 0.95$ (notice that half-filling corresponds to $n = 1$). As a second set of parameters we take a \mathbf{q} -dependent repulsion $J(\mathbf{q})$ (see Ref. 12) where $J(\mathbf{Q}) \equiv U = 3.3t$ (3.4*t*) and $\mu = -1.1$ ($n = 0.93$). The function $J(\mathbf{q})$ describes approximately the effect of vertex corrections and decreases as \mathbf{q} decreases from \mathbf{Q} to 0 (see Ref. 13). The superconducting coherence length ξ_0 at $T = 0$ is given by Eq. (9). For d -wave pairing ξ_0 decreases with increasing n and becomes about $\xi_0/a \approx 3$ near half-filling. For the relaxation time τ given by Eq. (10) we take as an upper limit the GLG value yielding $\tau\Omega = \pi\Omega/8T_c \approx 12(\Omega/t)$.

Quite generally we find that the dynamic spin susceptibility $\chi(\mathbf{q}, \omega)$ increases monotonically with decreasing T in the absence of order parameter fluctuations (OPFL's) while in the presence of OPFL's this function increases down to a crossover temperature T_* where it passes through a maximum, and then it decreases as T decreases from T_* downwards to T_c . In Figs. 2(a) and 2(b) we have plotted $\text{Im}\chi(\mathbf{Q}, \omega)$ versus ω for $U = 6t$, $n = 0.95$, $g = 4$, $\xi_0 = 1$, $\tau = 1$ and for $J(\mathbf{Q}) = U = 3.3t$, $n = 0.93$, $g = 1$, $\xi_0 = 4$, $\tau = 8$, respectively. The lowest line refers to $T = 0.04t$ [0.1*t* in (b)], and for decreasing T this function increases continuously up

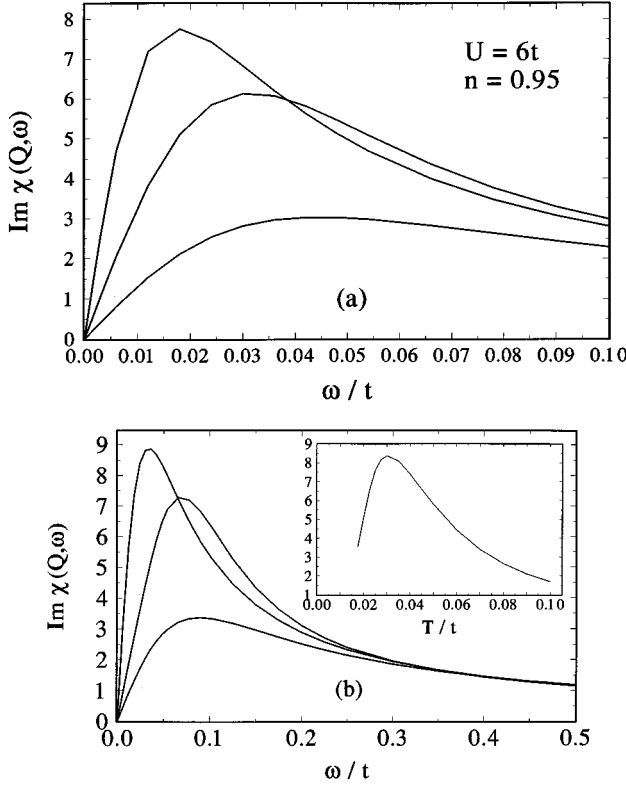


FIG. 2. Imaginary part of dynamical spin susceptibility, $\text{Im}\chi(\mathbf{Q}, \omega)$, at $\mathbf{Q}=(\pi, \pi)$, vs ω , in the presence of order-parameter fluctuations (OPFL's) with parameters g , ξ_0 , and τ . (a) $U=6t$, $n=0.95$, $g=4$, $\xi_0=1$, $\tau=1$, and temperatures $T=0.04t$ (lowest curve), $T=T_*=0.014t$ (uppermost curve), and $T=T_c=0.009t$ (intermediate curve). (b) $J(\mathbf{Q})=U=3.3t$, $n=0.93$, at $T=0.1t$ (lowest curve), $T=T_*=0.03t$ (uppermost curve), and $T=T_c=0.015t$ (intermediate curve). The inset shows this quantity for fixed $\omega=0.024t \approx 6$ meV as a function of T .

to the highest curve referring to the crossover temperature $T_*=0.014t$ [0.03t in (b)], and then it decreases continuously down to the intermediate curve referring to about $T_c=0.009t$ [0.015t in (b)]. One recognizes from Fig. 2 that the position ω_{sf} of the maximum of $\text{Im}\chi(\mathbf{Q}, \omega)$ decreases first with decreasing T down to T_* where it passes through a minimum, and then ω_{sf} increases as T decreases further towards T_c .

In the inset of Fig. 2(b) we have plotted $\text{Im}\chi(\mathbf{Q}, \omega)$ versus T at a fixed small value of ω ($0.024t \approx 6$ meV for $t=250$ meV). One sees that for decreasing T this function passes through a maximum at about T_* . This is in qualitative agreement with the neutron-scattering data on underdoped $\text{YBa}_2\text{Cu}_3\text{O}_{6+x}$ for $x=0.69, 0.83$, and 0.92 which have been interpreted to arise from the opening of a spin pseudogap.² One recognizes that the positions ω_{sf} of the maxima in Fig. 2(b) are much larger than in Fig. 2(a). The larger ω scales in Fig. 2(b) are in much better agreement with the neutron-scattering data than the small ω scales in Fig. 2(a).

An analogous temperature behavior is found for $\text{Re}\chi(\mathbf{q}, \omega)$ considered as a function of \mathbf{q} at fixed ω . For the same parameter values as in Fig. 2 we have plotted in Figs. 3(a) and 3(b) the function $\text{Re}\chi(\mathbf{q}, \omega=0)$ versus \mathbf{q} along a path in the Brillouin zone running from $\Gamma=(0,0)$ to

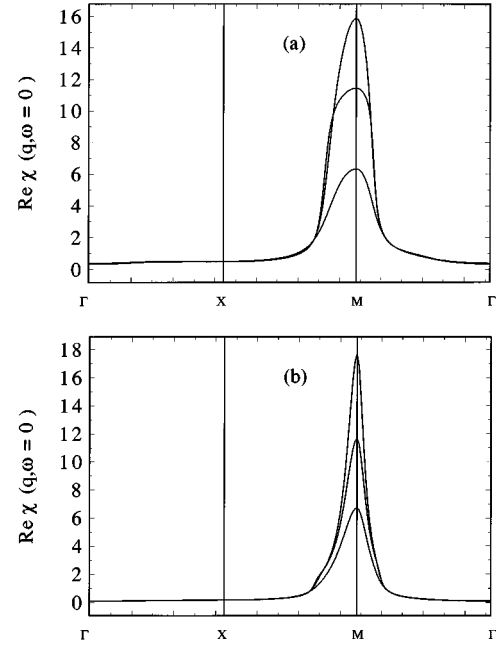


FIG. 3. Real part of dynamical spin susceptibility, $\text{Re}\chi(\mathbf{q}, \omega=0)$, vs \mathbf{q} along a path running from $\Gamma=(0,0)$ to $X=(\pi,0)$ to $M=(\pi,\pi)$ and back to Γ . (a) $U=6t$ and the same parameter values as in Fig. 2(a); (b) $J(\mathbf{Q})=U=3.3t$ and the same parameter values as in Fig. 2(b).

$X=(\pi,0)$ to $M=(\pi,\pi)$ and back to Γ . From the lowest solid line referring to $T=0.04t$ [0.1t in (b)] this function increases continuously for decreasing T up to the highest solid line referring to $T_*=0.014t$ [0.03t in (b)], and then it decreases continuously to the intermediate curve at about $T_c \approx 0.009t$ [0.015t in (b)]. One recognizes that the half-width of the peak, $\Delta q \sim \xi_{AF}^{-1}$, passes through a minimum at T_* for decreasing T . In the absence of OPFL's the height of the peak increases and the half-width Δq decreases monotonically with decreasing T .

These completely different behaviors of the temperature dependences of $\text{Im}\chi(\mathbf{Q}, \omega)$ and $\text{Re}\chi(\mathbf{q}, 0)$ in the absence or presence of OPFL's are reflected in the T dependences of the spin-lattice relaxation rate $1/T_1$ and of the spin-echo decay rate $1/T_{2G}$, respectively. Quite generally we can say that $1/T_1 T$ increases monotonically in the absence of OPFL's as T decreases down to T_c while it passes through a maximum at T_* with decreasing T in the presence of OPFL's. Thus $T_1 T$ has about the same T dependence as the spin fluctuation energy ω_{sf} . In Fig. 4 we have plotted some results for $1/T_1 T$ versus T down to T_c for $U=6t$ (a), $J(\mathbf{Q})=3.3t$ (b), and $J(\mathbf{Q})=3.4t$ (c), and for different parameter values of g , ξ_0 , and τ for the OPFL's. The Figs. 4(b) and 4(c) show that T_c and $1/T_1 T$ are suppressed by the order-parameter fluctuations in comparison to the values obtained without OPFL's. The suppression increases with the strength of the OPFL's where the latter increases with increasing coupling strength g and/or with decreasing coherence length ξ_0 and decreasing relaxation time τ . On the other hand, the position T_* of the maximum of $1/T_1 T$ increases with increasing strength of the OPFL's.

In Fig. 4(a) we show $1/T_1 T$ for $U=6t$, $n=0.95$, $\xi_0=1$,

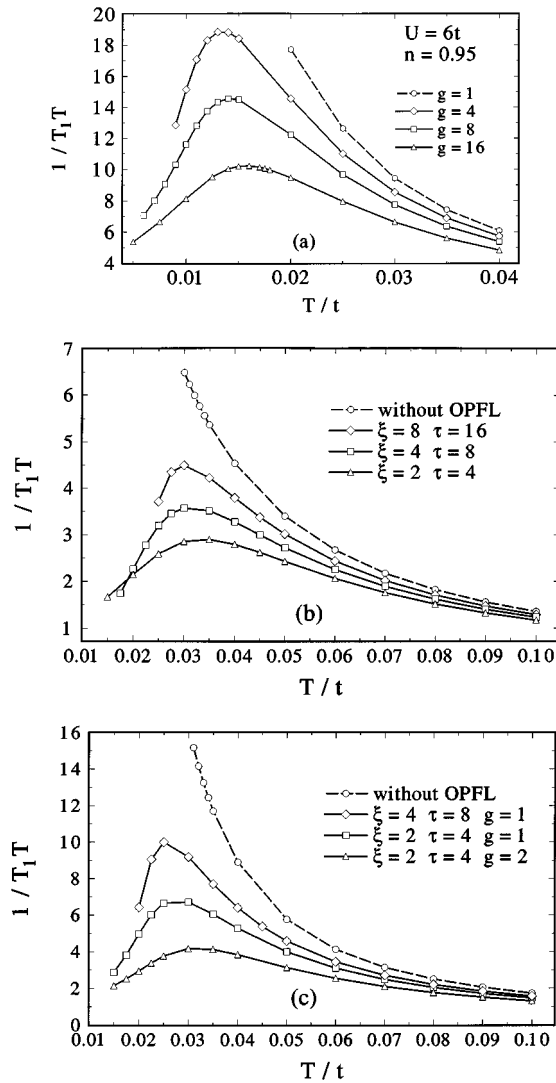


FIG. 4. The quantity $1/T_1T$ vs T where $1/T_1$ is the spin-lattice relaxation rate, for different coupling constants g , superconducting coherence lengths ξ_0 , and relaxation times τ of the order-parameter fluctuations. (a) $U=6t$, $n=0.95$; (b) $J(\mathbf{Q})=U=3.3t$, $n=0.93$; (c) $J(\mathbf{Q})=U=3.4t$, $n=0.93$.

$\tau=1$, and coupling constants $g=1, 4, 8$, and 16 (curves from top to bottom for this sequence of coupling constants). For $g=4, 8, 16$ we obtain the crossover temperatures $T_*/t=0.014, 0.015, 0.016$, and the $d_{x^2-y^2}$ -wave transition temperatures $T_c/t=0.009, 0.005, 0.001$. Thus T_c is strongly suppressed in comparison to the $T_{c0}\approx 0.018t$ without OPFL's. The relatively large values of the coupling constant g are in accordance with Eq. (11) because U is large ($U=6t$) and because the peaks of $\text{Re}\chi(\mathbf{q}, \nu)$ are large and have a relatively large half-width Δq [see Fig. 3(a)]. We have varied also ξ_0 and τ and find that $1/T_1T$ increases as ξ_0 and τ are increased. For example, by increasing ξ_0 and τ from 1 to 2 at fixed $g=8$ we obtain about the same curve in Fig. 4(a) as that for $g=4$, $\xi_0=1$, and $\tau=1$.

In Figs. 4(b) and 4(c) we show $1/T_1T$ for coupling $J(\mathbf{Q})$ with $J(\mathbf{Q})=U=3.3t$ ($3.4t$) and $n=0.93$. One recognizes that the temperature scales in Figs. 4(b) and 4(c) are much larger than those in Fig. 4(a) which is in much better agreement with the NMR experiments.^{1,3} For $J(\mathbf{Q})=U=3.3t$ [see

Fig. 4(b)] we obtain $T_{c0}=0.0304t$ without OPFL's, and $T_c/t\approx 0.024, 0.016$, and 0.01 for the sequence of parameter values $\xi_0=8, \tau=16, \xi_0=4, \tau=8$, and $\xi_0=2, \tau=4$ at fixed $g=1$. The values of T_*/t are in this sequence about $0.03, 0.032$, and 0.035 . For $U/t=3.4$ [see Fig. 4(c)] we obtain $T_{c0}=0.0314t$ without OPFL's, and $T_c/t\approx 0.019, 0.0125$, and 0.006 for the sequence of parameter values $\xi_0=4, \tau=8$ and $\xi_0=2, \tau=4$ at fixed $g=1$, and $\xi_0=2, \tau=4$ at $g=2$. The values of T_*/t in this sequence are about $0.025, 0.028$, and 0.032 . Our results in Fig. 4 show that for increasing U the strength of the spin fluctuations increases rapidly while their suppression due to coupling to order-parameter fluctuations increases rapidly with decreasing correlation length and relaxation time and/or increasing coupling strength g . For sufficiently large order-parameter fluctuations the crossover temperature T_* to spin pseudogap behavior can be much larger than T_c which agrees qualitatively with the NMR data on underdoped $\text{YBa}_2\text{Cu}_3\text{O}_{6+x}$ and $\text{YBa}_2\text{Cu}_4\text{O}_8$.^{1,3}

The calculated spin-echo decay rate $1/T_{2G}$ (with constant form factor) increases monotonically with decreasing T in the absence of order-parameter fluctuations while it passes through a maximum at T_* with OPFL's [see Fig. 5(a) for $U/t=3.3$]. Thus we can say that T_{2G} has about the same T dependence as the half-width $\Delta q \propto \xi_{\text{AF}}^{-1}$ of the commensurate peak [see Fig. 3(b)]. In Fig. 5(b) we have plotted the ratio T_1T/T_{2G}^2 versus T for $U/t=3.3$ and for the same parameter values as for $1/T_1T$ in Fig. 4(b). One sees that this ratio is nearly constant over the whole temperature region in the absence of OPFL's. Scaling arguments yield the relationship $T_1T/T_{2G}^2 = \text{const}$ for a dynamical scaling exponent $z=2$ corresponding to overdamped relaxational spin excitations.³ Such a behavior has been observed in overdoped cuprates.^{1,3} In Fig. 5(c) we have plotted our results for the other significant ratio T_1T/T_{2G} versus T for the same parameter values as in Fig. 5(a). One sees that without OPFL's this ratio decreases almost linearly with decreasing T . In the presence of OPFL's the curves for this ratio first run almost parallel to the former curve for decreasing T , then below a temperature of about T_{cr} these curves bend upwards until they reach a minimum at about T_* , and below T_* these functions increase rapidly as T decreases further towards T_c . Scaling arguments yield a relationship $T_1T/T_{2G} = \text{const}$ for a dynamical scaling exponent $z=1$ which applies to the quantum-disordered regime.³ Such a behavior has been observed in underdoped cuprates in a temperature region between T_{cr} and T_* .^{1,3} Our results in Fig. 5(c) show a constant behavior in the temperature region between T_{cr} and T_* to a very crude approximation.

We have seen in Figs. 4 and 5 that T_c is decreased and T_* is increased in proportion to the strength of the order parameter fluctuations. The latter are increased for decreasing ξ_0 and τ , or for increasing coupling constant g as can be seen from Eq. (14) for the fluctuation propagator K . According to the results of GLG theory⁷ ξ_0 and τ become smaller as the doping value away from half-filling, $x=1-n$, decreases. The question arises how the coupling constant g depends on doping x . As an example we have calculated g from Eq. (11) for fixed $U=3.3t$ and $T=0.03t$ and for two values of n , i.e., $n=0.83$ ($\mu=-1.35$) and $n=0.93$ ($\mu=-1.1$). We obtain $\text{Re}\chi(\mathbf{Q}, 0)\approx 7$ for $n=0.83$ and $\text{Re}\chi(\mathbf{Q}, 0)\approx 18$ for $n=0.93$;

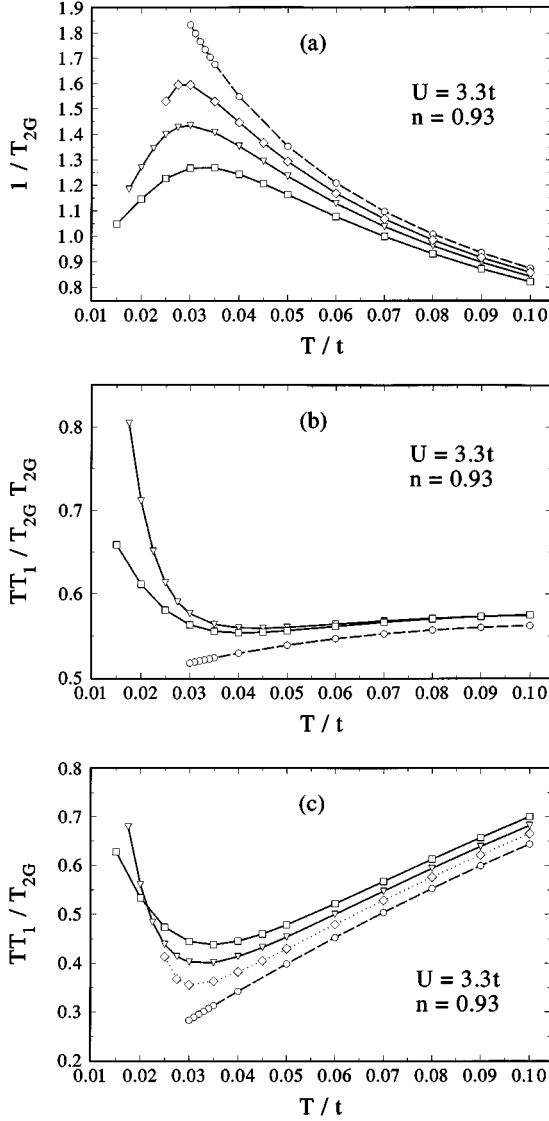


FIG. 5. Spin-echo decay rate $1/T_{2G}$ (a), ratio $T_1 T/T_{2G}^2$ (b), and ratio $T_1 T/T_{2G}$ (c), vs T , for $U=3.3t$ and $n=0.93$. The notations for the different parameter values of the order-parameter fluctuations are the same as those for $1/T_1 T$ in Fig. 4(b).

however, the half-width Δq of the commensurate peaks decreases as one goes from $n=0.83$ to $n=0.93$. Nevertheless, the coupling constant g is estimated to increase substantially as x decreases from $x=0.17$ to $x=0.07$.

A serious shortcoming of the previous FLEX approximation for spin fluctuations alone^{10–12} is that the T_c for $d_{x^2-y^2}$ -wave pairing increases monotonically with decreasing $x=1-n$. On the other hand, we have now shown that this T_c decreases with decreasing x since the strength of the order parameter fluctuations increases. These two opposite effects lead then to a maximum in T_c for decreasing x in qualitative agreement with experiment.

The reason that the spin susceptibility $\chi(\mathbf{q}, \omega) = \chi_0(\mathbf{q}, \omega)[1 - U\chi_0(\mathbf{q}, \omega)]^{-1}$ acquires a maximum at T_* for decreasing T (see Fig. 2) is that the irreducible susceptibility $\chi_0(\mathbf{q}, \omega)$ goes through a corresponding maximum. Indeed, the quantity $U_{cr} = [\chi_0(\mathbf{q}_c, 0)]^{-1}$ (where \mathbf{q}_c is the position of the maximum) passes through a minimum at T_* for decreasing

T while it decreases continuously towards U in the absence of OPFL's. The χ_0 is calculated from the quasiparticle spectral function $N(\mathbf{k}, \omega)$ (see Ref. 12) whose height and half-width at the Fermi momentum are given by $1/\Gamma(\mathbf{k})$ and $\Gamma(\mathbf{k})/\text{Re}Z(\mathbf{k}, 0)$, respectively, where $\Gamma(\mathbf{k}) = \lim_{\omega \rightarrow 0} \omega \text{Im}Z(\mathbf{k}, \omega)$ is the scattering rate. We find that in the absence of OPFL's the scattering rate Γ at the Fermi wave vector $\mathbf{k}_a = (0.172, 1)$ decreases linearly with T , while in the presence of OPFL's, Γ increases in comparison to the former one as T decreases below T_* . The effective mass ratio $\text{Re}Z(\mathbf{k}, 0)$ at \mathbf{k}_a increases slightly with decreasing T and has about the same value without and with OPFL's. The scattering rate Γ and the effective mass ratio $\text{Re}Z(\mathbf{k}, 0)$ at $\mathbf{k}_b = 0.406(1, 1)$ are about the same with or without OPFL's. Indeed, the peaks of $N(\mathbf{k}, \omega)$ for \mathbf{k} around \mathbf{k}_a are decreased and broadened (and shifted to lower ω) for $T < T_*$ while they are not affected around \mathbf{k}_b . Since $\chi(\mathbf{q}, \omega)$ depends very sensitively on $\chi_0(\mathbf{q}, \omega)$, and since the spectral function $N(\mathbf{k}, \omega)$ for \mathbf{k} near the antinode of the gap is decreased and broadened, one can understand that below T_* the susceptibility χ_0 is smeared out and in turn $\text{Im}\chi(\mathbf{Q}, \omega)$ decreases and $\text{Re}\chi(\mathbf{q}, 0)$ is broadened around $\mathbf{q} = \mathbf{Q}$.

Our theory cannot explain the observed crossovers of the in-plane resistivity and the uniform susceptibility for decreasing T in the underdoped cuprates. The calculated resistivity ρ is linear in T down to a low temperature T_0 ($\sim 0.02t$) and then bends upwards below T_0 like that observed in the overdoped regime. It is likely that the opposite behavior in the underdoped regime, i.e., a bending downwards of ρ below T_* , is caused by the Aslamazov-Larkin current contribution involving two fluctuation propagators.⁷ We obtain a slight decrease of the uniform and static spin susceptibility $\chi(0, 0)$ with decreasing T , however not such a drastic decrease below T_* as has been observed. This is plausible because the suppression of spin fluctuations by OPFL's is proportional to the strength of the spin fluctuations, and one sees from Fig. 3 that $\chi(0, 0)$ is much smaller than $\text{Re}\chi(\mathbf{Q}, 0)$. The vertex corrections due to spin fluctuations at $\mathbf{q} = 0$ are almost temperature independent¹³ which means that they cannot explain the drastic decrease of $\chi(0, 0)$ below T_* .

Another shortcoming of our theory is the fact that we do not find a quasiparticle gap in the spectral function $N(\mathbf{k}, \omega)$ as \mathbf{k} cuts through the Fermi line along the direction from $(0, \pi)$ to (π, π) as it has been observed above T_c in underdoped Bi 2212 (see Ref. 4). Notice that in the absence of OPFL's the peaks of $N(\mathbf{k}, \omega)$ for \mathbf{k} near the antinode \mathbf{k}_a of the gap are much smaller and broader than the peaks near the node \mathbf{k}_b of the gap. The OPFL's lead to an additional broadening of the peaks near \mathbf{k}_a and to shifts in ω of order $\omega \sim -0.03t$ which are similar to the observed ones.

IV. CONCLUSIONS

Our calculations show that inclusion of order parameter fluctuations in the FLEX approximation for the 2D Hubbard model is capable of explaining the spin gap properties of the high- T_c cuprates in the underdoped regime. These properties are determined by the dynamical spin susceptibility $\chi(\mathbf{q}, \omega)$ for wave vector \mathbf{q} near $\mathbf{Q} = (\pi, \pi)$. The underlying mechanism is a competition between spin fluctuations and order-

parameter fluctuations (OPFL's). The latter become sufficiently strong as T tends to T_c because the superconducting coherence length ξ_0 and the relaxation time τ due to pair breaking are relatively small for the high- T_c cuprates. The effect of OPFL's increases with decreasing doping away from half-filling, $x=1-n$, since on the one hand the coupling strength g increases, while on the other hand ξ_0 and τ decrease with decreasing x .

Our main result is that for sufficiently strong order parameter fluctuations the dynamic spin susceptibility $\chi(\mathbf{q}, \omega)$ passes through a maximum for decreasing T at a crossover temperature denoted by T_* . This leads to the spin gap behavior of three measured physical quantities. First, $\text{Im}\chi(\mathbf{Q}, \omega)$ at fixed small ω passes through a maximum at T_* for decreasing T [see Fig. 2(b)]. This result agrees qualitatively with the neutron scattering data on underdoped $\text{YBa}_2\text{Cu}_3\text{O}_{6+x}$ (see Ref. 2). Second, the antiparamagnon energy ω_{sf} corresponding to the position of the maximum of $\text{Im}\chi(\mathbf{Q}, \omega)$ passes through a minimum at T_* for decreasing T (see Fig. 2). This has the consequence that the spin-lattice relaxation rate divided by T , $1/T_1T$, passes through a maximum at T_* for decreasing T (see Fig. 4). Third, the half-width $\Delta q \sim \xi_{\text{AF}}^{-1}$ of the peak of $\text{Re}\chi(\mathbf{q}, \omega=0)$ at $\mathbf{q}=\mathbf{Q}$ passes through a minimum at T_* for decreasing T (see Fig. 3). This has the consequence that the spin-echo decay rate $1/T_{2G}$ passes through a maximum at T_* for decreasing T [see Fig. 5(a)]. The ratio T_1T/T_{2G}^2 is nearly constant as a function of T above a temperature $T_{\text{cr}} > T_*$ [see Fig. 5(b)] which means that one is in a dynamical scaling regime with exponent $z=2$ where the spin excitations are overdamped relaxational modes.³ The ratio T_1T/T_{2G} is approximately constant in the temperature region between T_{cr} and T_* [see Fig. 5(c)] which means that one is in a dynamical scaling regime with exponent $z=1$ (see Ref. 3). Our results for $1/T_1T$ and $1/T_{2G}$ in Figs. 4(b), 4(c), and 5 agree qualitatively with the NMR measurements in the overdoped and underdoped cuprates.^{1,3}

We find spin gap behavior for a large and constant on-site Coulomb repulsion ($U=6t$) as well as for a relatively small Coulomb repulsion $J(\mathbf{Q})$ [with $J(\mathbf{Q})=U=3.3t$] which decreases for $q \rightarrow 0$ to simulate the effect of vertex corrections.¹³ The latter interaction yields results for the neutron-scattering intensity and NMR relaxation rates which are in much better agreement with the experimental results¹⁻³ than those for $U=6t$ because the frequency and temperature scales, respectively, are much larger [compare Figs. 2(a) and 2(b), Figs. 4(a) and 4(b)]. Here it should be pointed out that our calculation of the spin susceptibility is formally inconsistent in our approximation for the self-energy because we have not calculated self-consistently the vertex corrections to the irreducible spin susceptibility which would be necessary for a conserving approximation. However, these vertex corrections are nearly temperature independent¹³ and therefore they should not contribute to the temperature crossover due to order-parameter fluctuations discussed in this paper.

The inclusion of order-parameter fluctuations in the FLEX approximation can explain also the observed doping

dependence of T_c . In the absence of OPFL's the T_c for $d_{x^2-y^2}$ -wave pairing increases monotonically with decreasing doping $x=1-n$ (see Ref. 12). Now we find that this T_c is suppressed in proportion to the strength of the OPFL's which increases with decreasing x . These two combined effects lead then to a maximum in T_c for decreasing x which agrees qualitatively with the doping dependence of T_c for the high- T_c cuprates. We have shown that on the other hand the crossover temperature T_* to spin gap behavior increases with increasing strength of the OPFL's and becomes much larger than T_c (see Figs. 4 and 5). This agrees with experiment.^{1,3}

It should be emphasized that the spin fluctuations and the order-parameter fluctuations are intimately coupled via the Eliashberg equations which contain the spin and order-parameter fluctuations as exchange interactions. The reason for the coupling is that these interactions are renormalized by the quasiparticle self-energy and by the superconducting eigenvalue λ_d and eigensolution ϕ_d , respectively. These quantities themselves are determined by the Eliashberg equations. For temperatures T sufficiently close to T_c the interaction due to order-parameter fluctuations can compete with the interaction due to spin fluctuations. This leads to a suppression of the maximum of the spectral density of the spin fluctuations, $\text{Im}\chi(\mathbf{Q}, \omega)$, as T decreases below the crossover temperature T_* . It is somewhat surprising that the eigenvalue $\lambda_d(T)$ for $d_{x^2-y^2}$ -wave pairing continues to increase up to unity as T decreases below T_* although the maximum of the pairing interaction, $(3/2)U^2\text{Im}\chi(\mathbf{Q}, \omega)$, decreases. The reason is that the decrease of the maximum of $\text{Im}\chi(\mathbf{Q}, \omega)$ below T_* is accompanied by an increase of its position ω_{sf} and a spread of this function to higher frequencies (see Fig. 2). It is well known that the larger the frequency spread of the pairing interaction the larger T_c or λ_d .

In summary, we have studied the effect of d -wave order-parameter fluctuations above T_c on spin fluctuations within an extension of the FLEX approximation for the 2D Hubbard model. Both kinds of fluctuations become very large for decreasing temperature T because one approaches the antiferromagnetic as well as the d -wave pairing instability. The crossover to spin gap behavior for decreasing T occurs at the temperature ($T_* > T_c$) where the quasiparticle interaction due to exchange of order parameter fluctuations becomes comparable to that due to spin fluctuations. The coupling of these fluctuations via self-energy renormalization gives rise to the observed spin gap behavior of the dynamic spin susceptibility $\chi(\mathbf{q}, \omega)$ for \mathbf{q} near the antiferromagnetic wave vector $\mathbf{Q}=(\pi, \pi)$. A shortcoming of the theory is that the effect of OPFL's cannot explain the observed spin pseudogap at $\mathbf{q}=0$ and the quasiparticle gap above T_c in underdoped cuprates. This raises the question of whether the latter gaps might have a different physical origin which is not described by the present FLEX approximation.

ACKNOWLEDGMENTS

We acknowledge helpful discussions with D.A. Fay. This work is supported by the Deutsche Forschungsgemeinschaft.

- *Present address: Department of Physics, University of California, Santa Barbara, California 93106-9530.
- ¹For a review see C.P. Slichter, in *Strongly Correlated Electronic Systems*, edited by K.S. Bedell *et al.* (Addison-Wesley, Reading, MA, 1994).
- ²For a review see L.P. Regnault *et al.*, *Physica B* **213-214**, 48 (1995).
- ³V. Barzykin and D. Pines, *Phys. Rev. B* **52**, 13 589 (1995); A.V. Chubukov, D. Pines, and B.P. Stojkovic (unpublished).
- ⁴D.S. Marshall *et al.*, *Phys. Rev. Lett.* **76**, 4841 (1996).
- ⁵S. Doniach and M. Inui, *Phys. Rev. B* **41**, 6668 (1990).
- ⁶V.J. Emery and S.A. Kivelson, *Nature* **374**, 434 (1995).
- ⁷L. Tewordt, D. Fay, and Th. Wölkhausen, *Solid State Commun.* **67**, 301 (1988).
- ⁸L. Tewordt, D. Fay, and D. Einzel, *J. Low Temp. Phys.* **21**, 645 (1975).
- ⁹N.E. Bickers, D.J. Scalapino, and S.R. White, *Phys. Rev. Lett.* **62**, 961 (1989).
- ¹⁰Chien-Hua Pao and N.E. Bickers, *Phys. Rev. Lett.* **72**, 1870 (1994).
- ¹¹P. Monthoux and D.J. Scalapino, *Phys. Rev. Lett.* **72**, 1874 (1994).
- ¹²T. Dahm and L. Tewordt, *Phys. Rev. Lett.* **74**, 793 (1995); *Phys. Rev. B* **52**, 1297 (1995); *Physica C* **246**, 61 (1995).
- ¹³T. Dahm and L. Tewordt, *Physica C* **265**, 67 (1996).